Europium- and Lithium-Doped Yttrium Oxide Nanocrystals that Provide a Linear Emissive Response with X-ray Radiation Exposure

Ian N. Stanton[§], Matthew D. Belley[‡], Giao Nguyen[◊], Anna Rodrigues[‡], Yifan Li[ø], David G. Kirsch[øΔ], Terry T. Yoshizumi[◊ø], and Michael J. Therien[§]*

[§]Department of Chemistry, French Family Science Center, 124 Science Drive, Duke University, Durham, NC 27708
[‡]Medical Physics Graduate Program, Hock Plaza, 2424 Erwin Road, Duke University, Durham, NC 27705
[◊]Department of Radiology, 2214 Elder Street, Duke University Medical Center, Durham, NC 27710
[ø]Department of Radiation Oncology, Box 91006, Duke University Medical Center, Durham, NC 27708
[Δ]Department of Pharmacology and Cancer Biology, Box 3813, Duke University School of Medicine, Durham, NC 27710.

Experimental:

Materials. $Y(NO_3)_3 \bullet 6H_2O$ (99.99%), $Eu(NO_3)_3 \bullet 5H_2O$ (99.9%), $Li(NO_3)$ (99.99%), and glycine (≥ 99%) were purchased from Sigma-Aldrich and used without further purification. HPLC-grade H_2O was also used (Fisher Chemicals).

Synthesis of [Y_2O_3; Ln]. [Y_2O_3; Eu_x], [Y_2O_3; $Eu_{0.1}$, Li_y], and [Y_2O_3; Li_y] compositions were synthesized by a solution combustion reaction involving glycine as the fuel. The reaction is as follows, where M = Y, Eu, or Li;

$$6\ M(NO_3)_3 + 10\ NH_2CH_2COOH + 18\ O_2 \rightarrow 3\ [M_2O_3] + 5\ N_2 + 18\ NO_2 + 20\ CO_2 + 25\ H_2O$$

The glycine-to-metal nitrate molar ratio was kept at 1.5:1 to ensure consistency of the samples. In a typical synthesis, 25 ml of HPLC grade H_2O was used to dissolve a total 0.2 mol/L of metal-nitrates and 0.3 mol/L of glycine in a 100 ml beaker. After stirring until dissolved fully, the stir-bar was removed and the reaction was placed on a hot plate set to maximum heat until combustion occurred. The hot plate and reaction beaker were enclosed in a plexi-glass box in a hood to limit airborne materials when combustion occurs. After the reaction, the beaker was immediately removed and allowed to cool to room temperature. Powders in the beaker and the enclosure were collected in an aluminum oxide crucible and placed in a furnace at 500 °C for 1 hour to burn off any residual nitrates. The powders were then experimentally tested as is.

Instrumentation:

X-ray Diffraction (XRD) and Transmission Electron Microscopy (TEM) were performed at the Shared Materials Instrumentation Facility (SMiF) at Duke University. Inductively Coupled Plasma Atomic Emission Spectroscopy (ICP-AES) was performed by Kim Hutchison at NC State University.

X-ray Diffraction. Powder XRD was measured on a Philips X'Pert PRO MRD HR X-Ray Diffraction System from 5° - 75° (2θ) under Cu K-Alpha (1.542 Å) irradiation at 45 keV and 40 mA.

Transmission Electron Microscopy. TEM was imaged on a FEI Tecnai G² Twin at a 200 keV accelerating voltage. Sample preparation consisted of making a 1 mg/mL solution of bare nanocrystals in ethanol, sonicating the solution for 1 minute in a bath sonicator, and then placing several drops of this solution on a carbon-formvar 400 mesh copper grid (EMS).

Raman Spectroscopy. The custom built Raman system utilized a PI Acton SP2360i 300 mm spectrograph outfitted with a PI Acton PIXIS 400 BR CCD detector. A Lasos 20 mW 633 nm He-Ne was utilized for sample excitation and its power density was controlled at 16 mW via a linear neutral density filter wheel. A Semrock RazorEdge Dichroic beam splitter and a Semrock Razor Edge long-pass laser blocking optics were employed to direct the excitation light to the sample and filter the laser's Rayleigh scatter from the Raman signal in the collection path to the detector.

UV-Excited Lifetime Spectroscopy. Solid-state lifetime traces were measured on an Edinburgh Instruments FLSP920 equipped with a Hamamatsu R2658 PMT and a micro-second flashlamp (pulsewidth ~2 μs), with excitation at approximately 255 nm and emission monitored at 611 nm. Steady-state excitation spectra were first recorded to identify the peak of the [Y_2O_3; $Eu_{0.1}$, Li_y] charge-transfer band at approximately 255 nm for flashlamp excitation. Each sample was prepared by placing 5 mg of nanocrystalline powder was placed in a solid-state powder cuvette (Starna), and mounted in a solid-state cuvette holder in the FLS920 sample chamber. Lifetimes were fit using the single exponential fitting program in the Edinburgh software.

Solid-state X-ray Excited Scintillation (XES). XES spectra were measured on an Edinburgh Instruments FLSP920 equipped with a Hamamatsu R2658 PMT over a 500 – 700 nm wavelength range. A Faxitron RX-650 X-Ray Cabinet fiber coupled (Ocean Optics 400 μm) to

the Edinburgh Instruments detection system allows for XES measurements with 130 kVp excitation power 130 kVp at a constant 5 mA. A X-Rad 320 X-Ray Cabinet fiber coupled (Ocean Optics 400 μm) to a Labsphere CDS2100 Spectrometer provided XES measurements at 40, 120, and 220 kVp (variable mA) over the range of 400 - 800 nm. For all measurements, 5 mg of [$Y_{2-x}O_3$; Eu_x, Li_y] nanocrystals were pressed into a 7 mm diameter pellet using a Pike Technologies' hand press, placed on a Teflon mount in the x-ray cabinet, and the fiber was mounted right next to the pellet for light collection. Emission intensity was maximized by fiber placement before the acquisition occurred for each powder sample in the same geometry.

Fiber-Optic Device XES Response. The fiber-optic device was made by pressing 1 mg of the [$Y_{1.9}O_3$; $Eu_{0.1}$, $Li_{0.16}$] material was into a 7 mm flat disk using the Pike Technologies' hand press to create a glass-like wafer. This wafer was then fractured into little pieces, where roughly a 400 μm diameter piece (~3.3 μg) of this wafer was optically-glued (Norland 81) to one end of a 400 μm (inner diameter) unjacketed optical fiber (Ocean Optics). Once the glue was UV-cured, the nanocrystal-based wafer was cracked to cover just the 400 μm optical fiber entrance without any overhang. The other end of the fiber was connected to a Princeton Instruments SP2360i 300 mm spectrograph with a Princeton Instruments Pixis 400BR CCD camera. Light collection was made from 585 - 645 nm on a high groove-density grating, where only the dominant 611 nm peak was integrated from 605 - 617 nm. The integration times of the CCD-camera were varied from 0.5 to 20 seconds at 80 and 225 kVp x-ray energies to record the total radiation exposure up to 6.4 Roentgen at 80 kVp and 117.8 Roentgen at 225 kVp.

Inductively Coupled Plasma Atomic Emission Spectroscopy (ICP-AES). ICP-AES measurements were made on a Perkin Elmer 2000 DV for Y, Eu, and Li ions in the as-synthesized samples. The data were compiled to compare the as-synthesized material to that anticipated based on reaction stoichiometry.

Figure S1. X-ray diffraction (XRD) spectra of the [$Y_{1.9}O_3$; $Eu_{0.1}$, Li_y] compositions. All material compositions display the cubic phase, space group Ia3, JCPDS-88-1040.

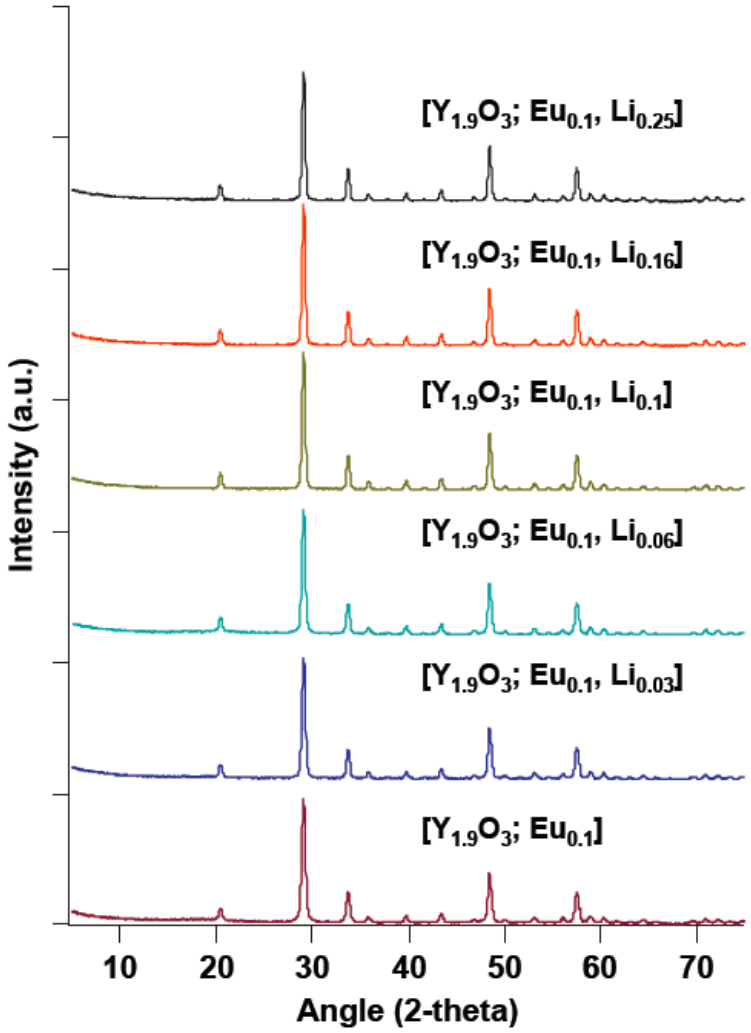

Table S1. ICS-AES compositional analysis of the [Y_2O_3; Eu_x], [Y_2O_3; $Eu_{0.1}$, Li_y], and [Y_2O_3; Li_y] samples, comparing the pre-combustion starting material predicted composition (theoretical) to the as-synthesized nanocrystal composition (actual). These data show that Eu ions are easily incorporated into the lattice with the anticipated stoichiometry; Li ion concentrations in the pre-combustion solution, however, exceed that found for the as-synthesized nanocrystals.

Theoretical	Actual
$[Y_2O_3]$	$[Y_2O_3]$
$[Y_{1.98}O_3; Eu_{0.02}]$	$[Y_{1.98}O_3; Eu_{0.02}]$
$[Y_{1.96}O_3; Eu_{0.04}]$	$[Y_{1.96}O_3; Eu_{0.04}]$
$[Y_{1.90}O_3; Eu_{0.1}]$	$[Y_{1.90}O_3; Eu_{0.1}]$
$[Y_{1.8}O_3; Eu_{0.2}]$	$[Y_{1.8}O_3; Eu_{0.2}]$
$[Y_{1.7}O_3; Eu_{0.3}]$	$[Y_{1.68}O_3; Eu_{0.32}]$
$[Y_{1.9}O_3; Eu_{0.1}]$	$[Y_{1.9}O_3; Eu_{0.1}]$
$[Y_{1.9}O_3; Eu_{0.1}, Li_{0.04}]$	$[Y_{1.9}O_3; Eu_{0.1}, Li_{0.03}]$
$[Y_{1.9}O_3; Eu_{0.1}, Li_{0.1}]$	$[Y_{1.9}O_3; Eu_{0.1}, Li_{0.06}]$
$[Y_{1.9}O_3; Eu_{0.1}, Li_{0.2}]$	$[Y_{1.9}O_3; Eu_{0.1}, Li_{0.1}]$
$[Y_{1.9}O_3; Eu_{0.1}, Li_{0.3}]$	$[Y_{1.9}O_3; Eu_{0.1}, Li_{0.16}]$
$[Y_{1.9}O_3; Eu_{0.1}, Li_{0.4}]$	$[Y_{1.9}O_3; Eu_{0.1}, Li_{0.25}]$
$[Y_2O_3; Li_{0.04}]$	$[Y_2O_3; Li_{0.03}]$
$[Y_2O_3; Li_{0.3}]$	$[Y_2O_3; Li_{0.18}]$

Figure S2. Additional TEM images of [$Y_{1.9}O_3$; $Eu_{0.1}$, Li_y] nanocrystals with increasing lithium-doping content. The amorphous content gradually disappears as Li ion concentration is increased; with these increasing Li+ concentrations, isolated nanoparticles feature larger diameters as well as more well-defined crystalline boundaries.

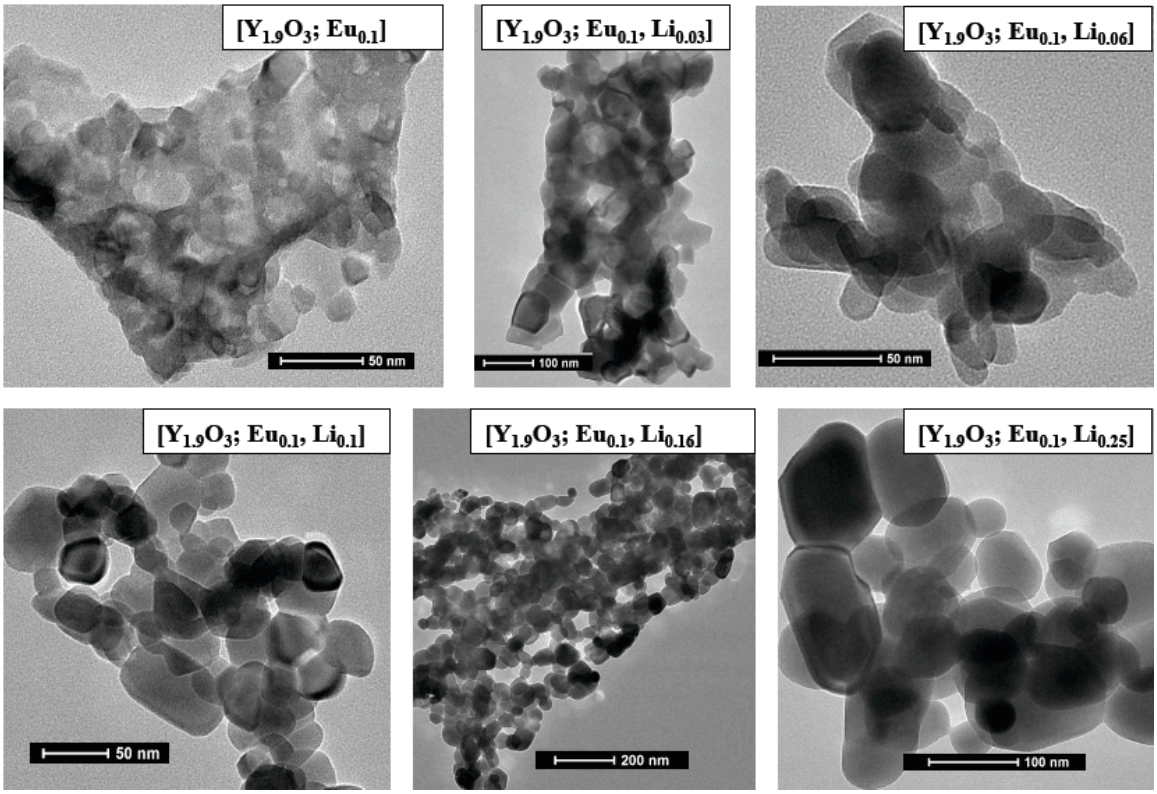

Figure S3. Normalized UV-excited lifetime traces for the [Y_2O_3; $Eu_{0.1}$, Li_y] samples monitored at 611 nm under flashlamp excitation of the [Y_2O_3; $Eu_{0.1}$, Li_y] charge-transfer band at approximately 255 nm. The lifetime measured for all samples is 2.12 +/- 0.04 ms via single exponential fitting.